Ratio Problem in Single Carbon Nanotube Fluorescence Spectroscopy

C. L. Kane and E. J. Mele

Department of Physics, Laboratory for Research on the Structure of Matter, University of Pennsylvania,
Philadelphia, Pennsylvania 19104, USA

The electronic band gaps measured in fluorescence spectroscopy on individual single wall carbon nanotubes isolated within micelles show significant deviations from the predictions of one electron band theory. We resolve this problem by developing a theory of the electron-hole interaction in the photoexcited states. The one-dimensional character and tubular structure introduce a novel relaxation pathway for carriers photoexcited above the fundamental band edge. Analytic expression for the energies and line shapes of higher subband excitons are derived, and a comparison with experiment is used to extract the value of the screened electron-hole interaction.

By isolating single wall carbon nanotubes (SWNT's) in micelles O'Connell *et al.* [1] have observed midinfrared fluorescence from individual SWNT's in solution. Measurements of the photoluminescence efficiency (PLE) as a function of the exciting optical frequency provide a useful probe of the optical excitations of individual SWNT's. These are of fundamental interest and provide a basis for applications of SWNT's as optical materials.

The spectra obtained in these experiments contain features not anticipated by existing models for the nanotube electronic structure [2–5]. In this Letter we study the "ratio problem"—the ratio between critical energies measured in these experiments violates a robust, model independent prediction of conventional one electron theory. Here we show that the ratio problem is resolved by identifying the effects of the electron-hole interactions in the optically excited states. The magnitude of this problem can be used to extract an experimental assignment of the strength of the screened Coulomb interactions between the excited electron and hole. We develop a model for the final state interactions following optical excitations into the higher subbands, and find that it contains several unique intrinsic relaxation mechanisms that derive from one dimensionality and tubular geometry of SWNT's. We estimate the intrinsic lifetime and derive an analytic expression for the line shape due to these processes.

The experiments of O'Connell *et al.* [1] measure absorption and fluorescence in solutions that contain micelles encapsulating single tubes of various radii and chiralities. The experimental situation is sketched in the left panel of Fig. 1, where optical excitation of an electron-hole pair into a high energy azimuthal subband (a) is followed by decay into the lowest subband from which the pair recombines with the emission of a photon (b). The band gaps depend on the tube radius and chirality. By measuring the dependence of the fluorescence at a *single* frequency on the exciting frequency, one isolates from the ensemble the electronic excitations of one (or possibly a few) tube wrappings. Thus, peaks in the PLE

can be assigned to electronic transitions between the quantized subbands of individual tubes.

The ratio of the frequency of the *second* peak in the PLE to the fluorescence frequency measures the ratio of the critical energies for excitations between the first two pairs of quantized azimuthal subbands of a single tube, as shown in Fig. 1. Crudely, the ratio of the second absorption frequency to the emission frequency should be two because of the quantization of the azimuthal component of the crystal momentum [2–5]. This prediction is not exact and is violated by effects arising from the tube curvature and from the threefold anisotropy (the so-called "trigonal warping") in the band structure [6]. However, these effects depend on the tube radius and vanish for large radius tubes. Thus one electron theory predicts that the frequency ratio must *asymptotically* approach two in the limit of large tube radius. Experimentally it does not, and instead approaches an asymptotic value nearer to 1.75. This is significant for the optical properties, and
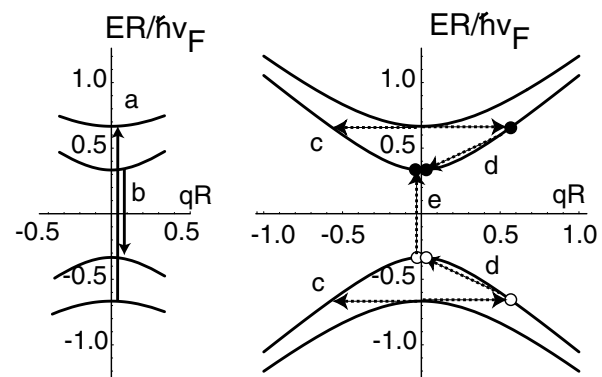

FIG. 1. Left: the excitation pathway leading to the ratio problem in SWNT fluorescence spectroscopy. Electron hole pairs excited into the second azimuthal subband (a) relax to the first azimuthal subband where they radiatively recombine (b). Right: the electron hole pair in the second subband can decay into a single electron hole pair in the first subband (c), or to a two electron–two hole state (d),(e)

corresponds to a shift of the expected locations of band edges as large as $2000\,\mathrm{cm}^{-1}$. We refer to this problem as the "ratio problem."

The ratio problem can be identified unambiguously by studying the asymptotic gap ratio in the limit of *large radius* tubes; the observed ratios for small radius tubes are sensitive to tube curvature and band structure anisotropy. However, even for small radius tubes the band model fails to describe the data since it predicts gap ratios larger than 2 for approximately half of the small radius tubes measured, contrary to experiment. Likewise, quasiparticle self-energy effects in the *single particle* Green's function do not resolve the ratio problem for large tube radii since the self-energy can be linearized in wave vector q close to the zone corner. Therefore the quasiparticle self-energy corrections also satisfy the asymptotic "ratio equals 2" rule for large radius tubes. As we show below the ratio problem can be traced to interaction effects in the electron-hole Green's function that persist in the large radius limit.

Previous measurements of the electronic spectra using single electron tunneling [7,8] have been interpreted within a conventional band picture including the effects of trigonal warping. However, unlike tunneling spectroscopy, optical excitation produces *two* charged carriers: the excited electron and its valence band hole which are bound by their Coulomb attraction [9] [Figs. 2(a) and 2(c)] producing an excitonic bound state. Our theory uses a variational method to study the long range interactions [Fig. 2(a)] that bind the exciton. For a nanotube of radius R embedded in a medium with dielectric constant κ it is convenient to introduce the energy parameter $\Delta = \hbar v_F/R$ where v_F is the Fermi velocity, and the dimensionless coupling constant $\tilde{\alpha} = \alpha/\kappa = e^2/(2\pi\kappa\hbar v_F)$. All energies in the problem can be expressed in units of Δ and $\tilde{\alpha}$ characterizes the strength of the screened Coulomb interaction. Our variational ansatz for the pair wave function for the nth subband exciton as a function of the relative coordinate $\Phi_n(\delta z) \sim \exp(-|\delta z|/\xi_n)$ gives an estimate of its localization length $\xi_n = 1.09\kappa R/n\alpha$ and binding energy $\delta E_n = 2.5n\alpha^2\Delta/\kappa^2$. Note that this binding energy scales with the size of the unrenormalized gap $2n\Delta/3$ and reduces its magnitude by $\approx 10\%$. For reasons discussed below, this result of the variational theory disagrees with the result of Ando's analysis of the exciton using a screened Hartree-Fock theory of the interaction [9]. While the electron-hole interaction reduces the observed thresholds for interband transitions, the binding energy scales with the subband index n and therefore this does not change the observed *ratios* of the intersubband transition energies. Since the width of this bound state can be much larger than a lattice constant we study the relaxation of the exciton in the Wannier limit.

Additionally, the Coulomb interaction mediates finite momentum *interband* relaxation processes that conserve the total crystal momentum [Fig. 2(b)]. These have an
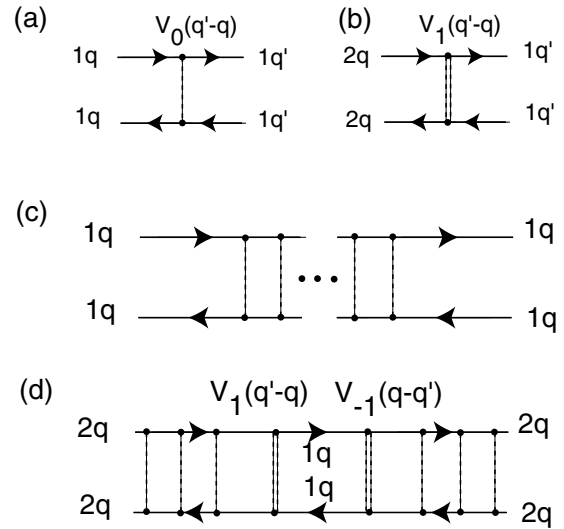

FIG. 2. The Coulomb interaction between the electron and hole is described by two fundamental scattering processes: (a) intraband scattering, conserving the azimuthal components of crystal momenta and (b) interband scattering with finite momentum transfer in the azimuthal direction. Interactions denoted by the dashed lines preserve the azimuthal crystal momentum; those denoted by double dashed lines carry one unit of the azimuthal crystal momentum $\hbar/R$. (c) is the multiple intraband scattering that leads to exciton formation and (d) describes the decay of the second subband exciton into electron hole pairs in the first subband.

unusual spectral structure because of the one dimensionality of the nanotube and the quantization of the azimuthal component of the crystal momentum.

An exciton created at the second subband edge can relax by decaying into an unbound electron-hole pair in the first subband with nonzero kinetic energy [as shown in process (c) of Fig. 1]. This process transfers one unit of azimuthal crystal momentum from the electron to the hole. The decay rate can be calculated using the golden rule which gives the second subband exciton a self-energy

$$\Sigma_2(E) = \lim_{\delta \to 0} \frac{\tilde{\alpha}^2 \hbar v_F}{R} \int d\zeta \, \frac{|V_1(\zeta)|^2 |M_{21}(\zeta)|^2}{(E + i\delta)/\Delta - 2\sqrt{(1/3)^2 + \zeta^2}}$$

$$= iA(E)\tilde{\alpha}^2\Delta, \tag{1}$$

where the momentum transferred in the scattering $q = \zeta/R$, $V_1(\zeta) = 2I_1(\zeta)K_1(\zeta)$ is the Coulomb kernel for interband scattering at wave vector ζ along the tube axis expressed in terms of the Bessel functions of imaginary argument I_m and K_m, and M_{21} is the scattering matrix element evaluated in the effective mass theory [10]. Integrating Eq. (1) we find $A(4\Delta/3) \approx 2.3$.

A remarkable feature of the nanotube electronic spectrum is that the interband excitations in the second subband have sufficient energy to decay into *pairs* of first subband particle hole excitations as depicted in Figs. 1(d) and 1(e). A typical process that contributes to this decay is

shown in Fig. 3(a) where a hot electron excites a second electron-hole pair. (There are three related though inequivalent processes that are not shown in this figure.) The amplitudes for these processes first appear in the perturbation theory at order $\tilde{\alpha}^2$.

All the scattering processes that contribute to this relaxation channel are constrained by conservation of crystal momentum so that the four momenta in the final state of Fig. 3(b) sum to zero. At the low energies relevant to our problem the situation is further simplified by projecting this amplitude onto the final state containing a pair of first subband excitons with momenta $\pm Q$. The projection is carried out by integrating over the two relative momenta of the bound electrons and holes, so that the phase space for the final state is *one dimensional* indexed by the single remaining free momentum Q. Thus the spectral weight for these final states diverges at low energy proportional to $1/\sqrt{E}$. This leads to the unusual situation sketched in the inset to Fig. 4. The electron-hole excitation at the second band edge resonates with a nonsingular background of electron-hole excitations from the lowest azimuthal subband [this is described by the self-energy of Eq. (1)] and hybridizes with the two electron–two hole continuum that has a *one-dimensional singularity* at its threshold.

The vertex function $\Gamma(q_2, q_1, q_1', q_1'')$ for this latter process depends only weakly on the momenta over the width ξ^{-1} relevant to describe the Wannier exciton. Using this fact we obtain

$$\Gamma = \frac{\tilde{\alpha}^2 \hbar v_F}{R} \int_{-\Lambda}^{\Lambda} d\zeta \, \frac{V_1(\zeta) V_0(\zeta) M_{2111}(\zeta)}{2/3 - \sqrt{(1/3)^2 + \zeta^2}} = B\tilde{\alpha}^2 \Delta e^{i\theta}, \quad (2)$$

where $V_m(\zeta)$ gives the Coulomb kernels for scattering with m units of crystal momentum in the azimuthal direction and with $\delta q = \zeta/R$ along the tube axis. The factor M in the integrand is a matrix element that we evaluate using the single particle states in the effective

mass wave functions on the tube [10]. Λ is an ultraviolet cutoff on the integral for which a Debye approximation gives the estimate $\Lambda \approx 2.7$. The integration in Eq. (3) then gives $B \approx 5.83$ and yields for the self-energy of Fig. 3(c)

$$\Sigma_4(E) \approx \frac{\tilde{\alpha}^4 B^2 \Delta}{\sqrt{(4/3)^2 - (E/\Delta)^2}}. \quad (3)$$

Combining the results of Eqs. (1) and (3) we obtain an expression for the exciton Green's function in terms of the scaled energy $\varepsilon = E/\Delta$

$$G(\varepsilon) = \frac{1}{\varepsilon - \varepsilon_o + iA\tilde{\alpha}^2 + B^2 \tilde{\alpha}^4 / \sqrt{\varepsilon_o^2 - \varepsilon^2}}, \quad (4)$$

where ε_o gives the (scaled) energy of the unperturbed exciton. The absorption line shape $\mathcal{L}(\varepsilon) = -\text{Im}\, G(\varepsilon)/\pi$
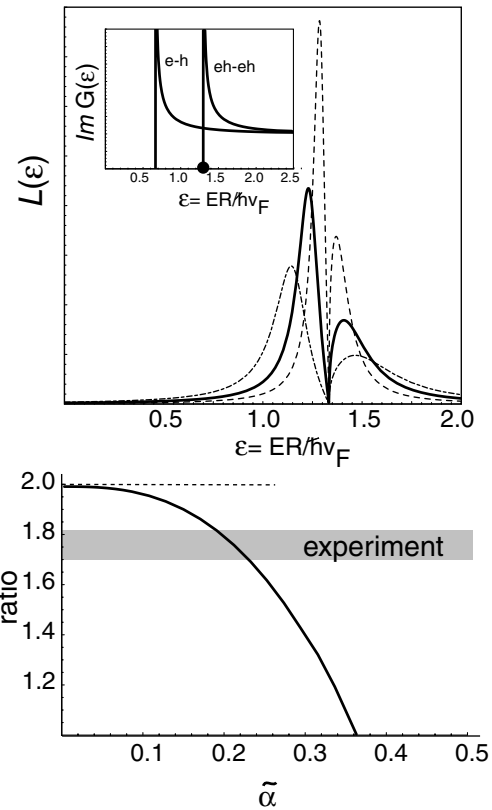
FIG. 4. Absorption line shapes for the second subband exciton resonating with first subband excitations plotted as a function of the dimensionless energy $\varepsilon = ER/\hbar v_F$. The inset shows the spectral densities for the electron-hole and two electron–two hole continua. The bold dot denotes the location of the unrenormalized second subband exciton. The curves show the dimensionless line shapes computed from Eq. (4) for three values of the screened dimensionless coupling constant of the theory [$\tilde{\alpha} = 0.15$ (dashed), 0.20 (solid), 0.25 (dot-dashed)]. The lower panel gives the ratio of the energy of the renormalized exciton to the energy of the fluorescence. The unrenormalized theory gives the dashed line and the shaded region is obtained from the experiments of Ref. [6].
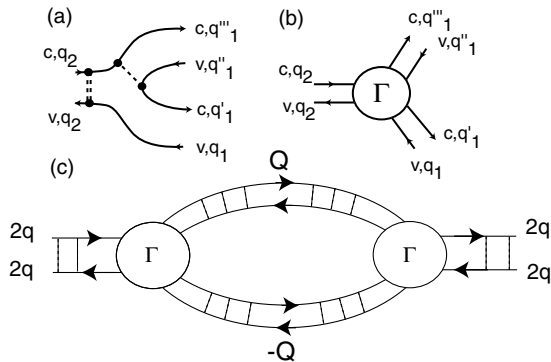
FIG. 3. An electron hole pair in the second azimuthal subband can relax into a final state containing two electrons and two holes: (a) A typical amplitude for this relaxation process; (b) the general vertex for the relaxation; (c) the exciton self-energy produced by this process.

is therefore completely determined by the screened coupling constant $\tilde{\alpha}$; in Fig. 4 we plot $\mathcal{L}(\varepsilon)$ for three representative values of the coupling. The zero in this line shape denotes the locations of the threshold energy for the two particle–two hole continuum. Note that while the electronic band gaps depend on tube radius R, scaling approximately as $1/R$, the Coulomb interaction has the same scaling with radius. In particular, for large radius tubes the excitonic interactions become weak *in proportion* to the scale of the band gap, expressed as a fraction of the band gap it approaches a nonzero limit for large R.

The second term in the self-energy of Eq. (4) is higher order in the small parameter $\tilde{\alpha}$, but it makes a significant contribution to the self-energy because of its singular energy dependence. Solving for the roots of the denominator we find that the pole for the bare second subband exciton is shifted to lower energy $\Delta\varepsilon = -3^{1/3}B^{4/3}\tilde{\alpha}^{8/3}/2$ and develops a width $\delta\varepsilon = A\tilde{\alpha}^2$. In contrast, the first subband exciton is unaffected by any similar relaxation process, since it does not overlap a pair continuum, and therefore it is unrenormalized.

In the lower panel of Fig. 4 we plot the ratio of the renormalized energy of the second subband exciton to the energy of the first subband exciton. The dashed line gives the result of the noninteracting theory that ignores these relaxation effects. Experiment indicates that in the limit of large tube radii the ratio lies in the shaded region, which is well described by a dimensionless coupling constant $\tilde{\alpha} \approx 0.20$. The *unscreened* coupling constant is $e^2/2\pi\hbar v_F \approx 0.42$ and so the fit indicates an effective dielectric screening of the exciton with $\kappa \approx 2.1$. For this coupling constant the linewidth is $\approx 0.09\hbar v_F/R$, giving $\delta\lambda/\lambda \approx 0.07$ which is quite close to the experimentally observed width in PLE [6]. This coupling constant places the nanotube micelle in the crossover regime where the shift and width of the line are comparable, as shown as the bold curve in Fig. 4.

A single electron injected into the second azimuthal subband edge has insufficient energy to relax by exciting an electron-hole pair. Thus the processes illustrated in Fig. 3 for the exciton do not occur in the single particle Green's function and should have no effect on electronic spectra measured by tunneling spectroscopy.

The effect of the Coulomb interaction on the optical excitations has been studied theoretically previously by Ando [9]. His work augments the effective mass model by introducing a Coulomb interaction between electrons that is studied within the Hartree-Fock approximation. Ando's approach predicts an enhancement of the single particle band gap due to the interactions, and the appearance of a bound exciton spectrum within this larger gap. Note, however, that the effective mass Hamiltonian is parametrized to match the low lying quasiparticle excitations of a the reference graphene sheet and thus already includes some self-energy effects due to the Coulomb

interaction. Our model treats the excitonic effects of the Coulomb interaction between the electron and hole, and therefore builds in the correct separation energy within the effective mass theory. Processes leading to the self-energy of Fig. 3 occur beyond the level of a Hartree-Fock treatment of the interaction.

It is interesting that if the coupling constant $\tilde{\alpha}$ were unscreened, the renormalized second subband exciton hybridizes so strongly with the two electron–two hole continuum that its energy becomes comparable to that of the fundamental first subband exciton. This situation is reminiscent of the known anomalous ordering of the electronic excitations of the polyenes [11]. There the lowest singlet excitation corresponds not to the promotion of a single electron from the highest occupied molecular orbital to the lowest unoccupied molecular orbital, but instead to a two particle–two hole excited state.

The interaction of carbon nanotubes with visible light results in the formation of "hot" carriers well above the lowest band edge. Our results demonstrate that a quantitative analysis of these excitations requires an understanding of the dominant relaxation mechanisms for these carriers. We find that the excitations of the many body system at these energies mix the interband excitations of the independent particle model with a continuum of primitive electron-hole excitations, and the latter are particularly strong because of the one-dimensional character of these structures. These can now be included in quantitative analyses of spectroscopic data on these systems.

---

[1] M. J. O'Connell *et al.*, Science **297**, 593 (2002).

[2] M. S. Dresselhaus, G. Dresselhaus, and P. C. Eklund, *Science of Fullerenes and Carbon Nanotubes* (Academic, San Diego, 1996).

[3] N. Hamada, S. Sawada, and A. Oshiyama, Phys. Rev. Lett. **68**, 1579 (1992).

[4] J. W. Mintmire, B. I. Dunlap, and C. T. White, Phys. Rev. Lett. **68**, 631 (1992).

[5] R. Saito, M. Fujita, G. Dresselhaus, and M. S. Dresselhaus, Appl. Phys. Lett. **60**, 2204 (1992).

[6] S. M. Bachilo *et al.* Science **298**, 2361 (2002).

[7] J. W. G. Wildoer *et al.*, Nature (London) **391**, 59 (1998).

[8] T. W. Odom *et al.*, Nature (London) **391**, 62 (1998).

[9] J. Ando, J. Phys. Soc. Jpn. **66**, 1066 (1997).

[10] C. L. Kane and E. J. Mele, Phys. Rev. Lett. **78**, 1932 (1997).

[11] P. Tavan and K. Schulten, Phys. Rev. B **36**, 4337 (1987).